

Vorticity in the Wake of a Small Horizontal Axis Wind Turbine

Paul R. Ebert and David H. Wood
Department of Mechanical Engineering
The University of Newcastle
Callaghan, New South Wales 2308
Australia

ABSTRACT

The three-dimensional structure of the mean vorticity in the wake of a horizontal-axis wind turbine was determined using hot-wire anemometry and the technique of phase locked averaging. Measurements were made at six axial locations in the near-wake, and for three values of the tip speed ratio, representing below-, near-, and above-optimum performance. The discussion focuses on the behaviour of the tip vortex which is shown to be characterised by high levels of streamwise velocity within its core.

INTRODUCTION

This paper presents three-dimensional measurements in the wake of a small horizontal axis wind turbine (HAWT); specifically we consider the development of the mean vorticity. This has a significant effect on the flow through the blades and hence performance, but very little is known about its detailed structure. In fact, there are no comprehensive data available for wind turbine wakes in general, and tip vortex structure in particular. This is in contrast to the situation for hovering rotors, eg Langrebe (1972), and propellers, eg Favier et al. (1989). Indeed, it is only very recently that measurements of the pitch of the tip vortex have become available, Ebert & Wood (1994). Computational wake models generally make assumptions about the wake that become less accurate for tip speed ratios ($\lambda \equiv R\Omega/U_\infty$) greater than that giving optimum performance; here R is turbine radius (= 250 mm in the present case), Ω is turbine rotational speed and U_∞ is the wind speed.

A special reason for studying the tip vortex is its importance as the turbine approaches runaway, where no net power is produced but the tip speed ratio is maximised. Runaway cannot be predicted by conventional wake models which ignore the structure of the tip vortex and the three-dimensionality of the whole flowfield. Wood (1993, 1994) suggested that runaway occurs when the tip vortex absorbs all the momentum,

angular momentum, and energy that would otherwise be extracted from the flow. To do this, the vortex must have structure; its core size must be significant as must U_a , the velocity in the direction of the vortex axis. Wood (1993) re-derived the energy and momentum equations for a wind turbine (at high λ) in a manner that accounted for the three-dimensionality of the flow. He found that U_v - the streamwise velocity of the vortex core - entered the equations. This velocity, in turn, is partially set by the vortex structure because the binormal velocity, W_a , which contributes significantly to U_v , receives a contribution from U_a , the velocity in the direction of the vortex according to the Widnall & Bliss (1971) equation:

$$\delta W_a = \pi a^2 U_a^2 / (r \Gamma) \quad (1)$$

where r is the vortex radius, a its diameter, and Γ its circulation. The simple-minded explanation of Equn (1) is that the centrifugal force associated with a uniform axial velocity of a curved vortex line must be balanced by a component of the Kutta-Joukowski lift ($\rho \delta W_a \Gamma$) which, in turn, alters the binormal velocity in a manner that does not depend on the sign of U_a .

In setting up the experiment, we were forced to use a wind tunnel whose outlet radius was equal to R . Thus we restricted all measurements to within two chord lengths of the blade and so the concentrated on measuring the development of the near-wake. Particular attention was paid to the tip and hub vorticities, for λ at and away from optimum. General comments on other features of the vortex structure are also given mainly in terms of the velocities of the vortex cores.

EXPERIMENTAL DETAILS

The two bladed HAWT, described by Ebert & Wood (1994), and in more detail by Ebert (1995), was placed at the exit of a wind tunnel. The three mean velocities and six Reynolds stresses were measured in the wake using

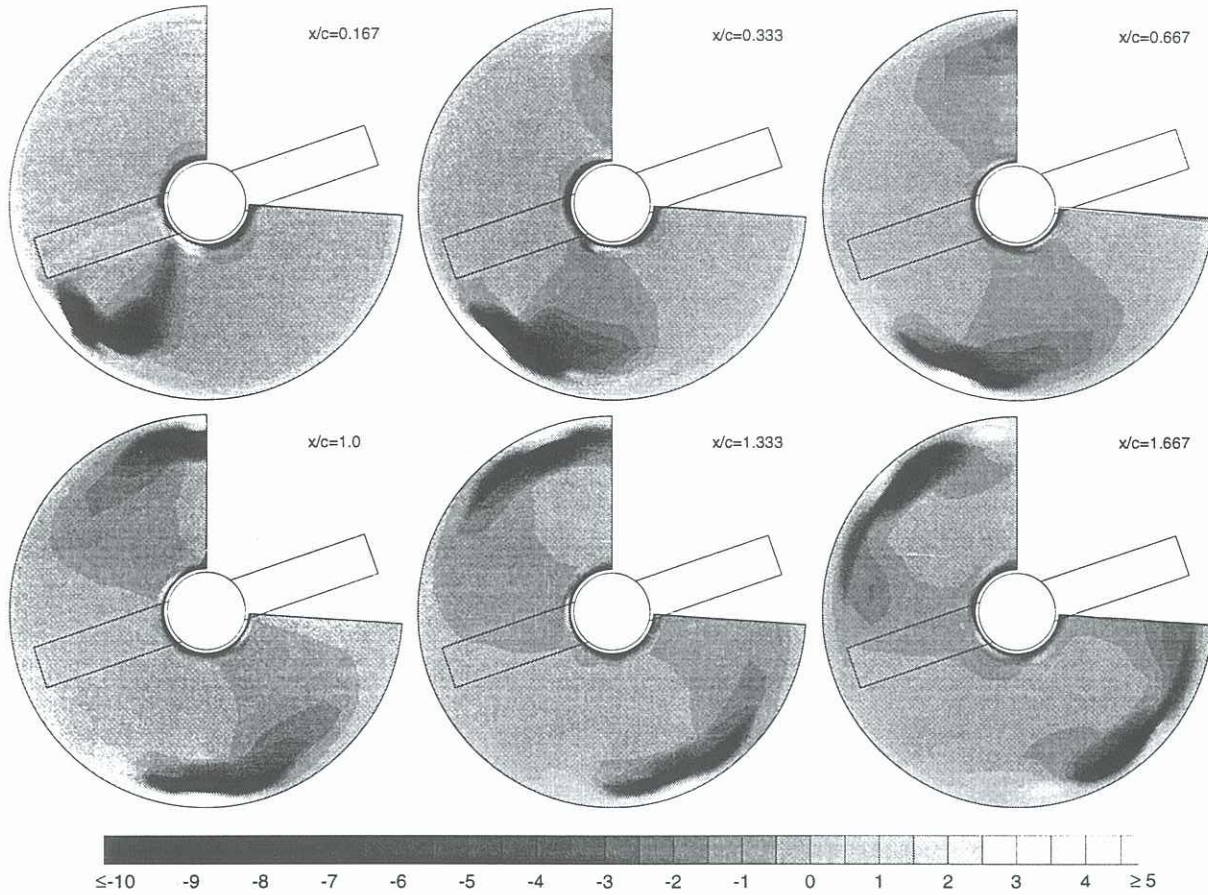


Figure 1. Contours of normalised circumferential vorticity, $\Omega_p R/U_\infty$, for $\lambda = 4$, and $C_p = 0.39$. Contour levels indicated in figure.

constant temperature anemometers with X-probes. Data were acquired by a 12 bit analog to digital board after the probe was positioned by a stepper motor traverse system. All traverses were radial, and by using the method of phase locked averaging (PLA), the full three-dimensional flow field was determined. PLA consists of triggering the data sampling whenever a blade passes a particular but arbitrary point. A number of samples are then collected at a fixed sampling rate, and by repeating the process and ensemble averaging over a large number of revolutions, the three-dimensional mean and turbulent flow field is approximated. In our experiments, averaging was over 6000 revolutions. Experiments were conducted for $\lambda = 2, 4$ and 6 at nominal axial positions, $x/c = 0.17, 0.33, 0.67, 1.0, 1.33$ and 1.67 , where x is measured from the blade trailing edge, and c ($= 60$ mm) is the blade chord. At each x , fourteen radial positions, from $r = 60$ mm to 280 mm were used. The centrebody radius was 55 mm. One λ , one x and the 14 radial positions made up one individual experiment. For $\lambda = 2, 4$ and 6 , respectively; $90, 70$ and 55 PLA measurements over $300^\circ, 270^\circ$ and 220° were obtained for each experiment. Finally, using a specially built dynamometer, the power extracted by the turbine was measured resulting in power coefficients (C_p) of $0.13, 0.39$ and 0.29 for $\lambda = 2, 4$ and 6 , respectively.

The three mean velocities, (U, V, W) , were obtained in polar cylindrical coordinates; U is the streamwise (x)

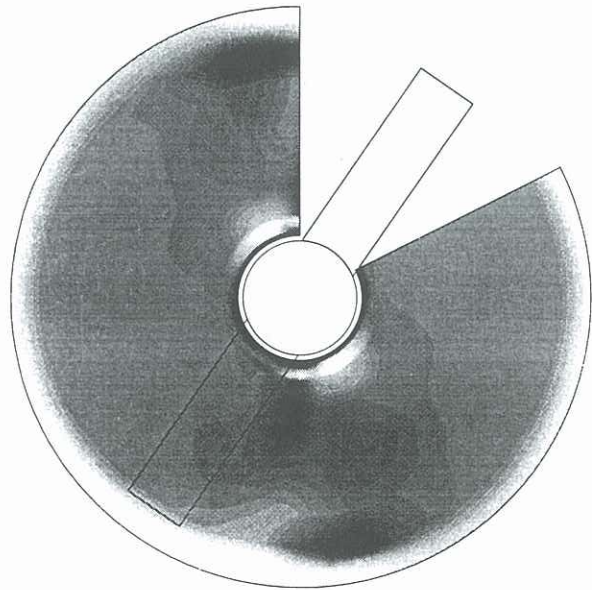


Figure 2. Contours of normalised circumferential vorticity, $\Omega_p R/U_\infty$, for $\lambda = 2$, $x/c = 1.0$ and $C_p = 0.13$. Contour levels as in Figure 1.

velocity, and V and W are the radial (r) and circumferential (θ) velocities respectively. The velocity gradients comprising the vorticity components were approximated by using (mainly) central differences.

RESULTS

For brevity, only the results for $\lambda = 4$ will be presented for all six axial locations; this λ gave the highest C_p and should be most applicable to operating turbines. Figure 1 shows the downstream development of Ω_θ , which is the major contributor to the vorticity in the direction of the vortex axis. The last two parts of Figure 1 indicate that the symmetry in the experimental results is very good. As a comparison, Figure 2 and 3 show Ω_θ for $\lambda = 2$ and 6 respectively at $x/c = 1$. In all figures, the flow is into the page, with the blade position indicated. The blades rotate clockwise.

Results for $\lambda = 4$ were generally as expected, with a well defined helical vortex structure close to the tip, and one opposite in sign but much less delineated near the hub. Part of the reason for this was the inability to measure closer than 5 mm to the centrebody. The pitch of the tip vortex was proportional to λ , (see Ebert & Wood (1994) for more details), and larger for the tip than hub vortex, and the helices were anti-clockwise. Because the results are for constant x/c , the vortices appear elongated, with the extent increasing with λ . The radius of the tip vortex also increased with λ . For all λ , the flow was complicated close to the blades, with many regions of both negative and positive vorticity, though by $x/c = 1$ a more coherent structure was usually evident. At $\lambda = 2$, however, there were vortex interactions that continued through the measured range of x/c , resulting in a number of vortices, partially evident in Figure 2, which may be the result of blade stalling. For $\lambda = 6$, a strong tip vortex was found, clearly evident in Figure 3, but the hub vortex became almost unidentifiable by $x/c = 1$.

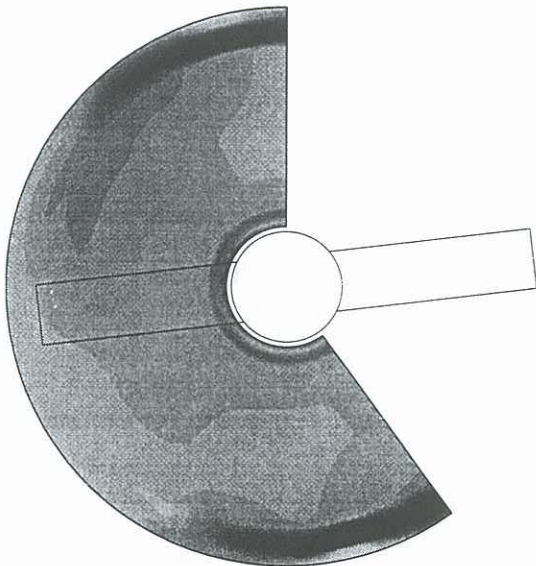


Figure 3. Contours of normalised circumferential vorticity, $\Omega_\theta R/U_\infty$, for $\lambda = 6$, $x/c = 1.0$ and $C_p = 0.29$. Contour levels as in fig. 1.

To concentrate on the tip vortices, the planar data was transformed into "vortex" co-ordinates using the measured pitch. The vortex axis was assumed to lie in the direction of the pitch and the measurements were assumed to be at the same axial location, even though the X-probe cut the vortex at large angles. For that reason, the transformation, which is similar to that used Thompson et al. (1990), is not globally valid. Typical results, for $\lambda = 4$ at the largest x/c , are shown in figure 4. It shows contours of Ω_a - the vorticity in the direction of the vortex axis. The tip vortex is not circular, and appears to have a leg that connects with the predominantly radial vorticity in the blade wake. Furthermore, the vortex is large, with a "diameter" of around $0.1R$ or $0.5c$. Figure 5 shows U_a and W_a for all tip speed ratios. The latter is the binormal velocity, which contributes significantly to U_a , the vortex velocity in the streamwise direction. The generally large magnitude is, presumably, an indication of the Kutta-Joukowski forces acting on the vortices to cause them and the wake to expand.

If all the quantities in Equn (1) are normalised by R and U_0 ; $a \sim 0.1$, $r \sim 1$ from Figure 5, and $\Gamma \sim \lambda^{-1}$, Wood (1993). Taking a generous estimate of 0.5 for U_a gives $\delta W_a \sim 0.05$ which is negligible. It appears, therefore, that λ is not sufficiently high for there to be a significant effect of the vortex structure on the conservation equations. The results, however, give some support to

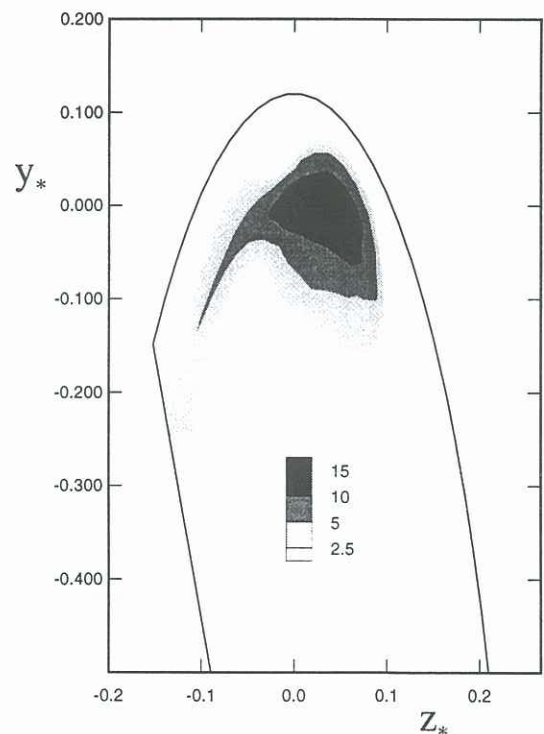


Figure 4. Contours of normalised vorticity in the direction of the vortex axis, $\Omega_a R/U_\infty$ for $\lambda = 4$, $x/c = 1.67$. Contour levels indicated in table. y_* and z_* have their origin at vortex centre, and are normalised by R . The algorithm to select the vortex centre has chosen the vortex at the bottom right of the contours shown in Figure 1.

the idea that U_a becomes increasingly negative as λ increases and eventually contributes significantly to W_a .

CONCLUSIONS

We have demonstrated that the process of trailing vortex formation behind a horizontal-axis wind turbine is a complex one. Only the optimum tip speed ratio gave a wake that was conventional in that the tip vortex formed quickly and was always identifiable as a single vortex. For all tip speed ratios, however, the vortex structure simplified quickly with downstream distance, so that by about two chord lengths from the blades, an identifiable tip vortex was present. This vortex is, however, not circular and its typical dimension is not small in comparison to the blade chord or tip radius. Although the spatial resolution is poorer near the hub, it appears that the hub vorticity does not reside in a coherent vortex, but more in sheet form. Further analysis is underway on the hub vortex as well as further analysis of the turbulence in the blade wakes and the behaviour of the mean velocity fields.

ACKNOWLEDGEMENTS

This work was supported by the Australian research Council and was done while PE held an Australian Postgraduate Research Award.

REFERENCES

- Ebert, P.R., 1995, Ph.D. thesis, Univ. Newcastle, in preparation.
- Ebert, P.R., and Wood, D.H., 1994, "Three dimensional measurements in the wake of a wind turbine, *European Wind Energy Conf.*, Thessalonika.
- Favier, D., Ettaouil, A., and Maresca, C., 1989, "Numerical and experimental investigation of isolated propeller wakes in axial flight", *Journal of Aircraft*, Vol. 26, pp. 837 - 846.
- Langrebe, A.J., 1972, "The wake geometry of a hovering helicopter rotor and its influence on rotor performance", *Journal of the American Helicopter Society*, Vol. 17, pp. 3 - 15.
- Thompson, T.L., Komerath, N.M., and Gray, R.B., 1988, "Visualisation and measurement of the tip vortex core of a rotor blade in hover", *Journal of Aircraft*, Vol. 25, pp. 1113 - 1121.
- Widnall, S.E., and Bliss, D.B., 1971, "Slender-body analysis of the motion and stability of a vortex filament", *Journal of Fluid Mechanics*, Vol. 50, pp. 335 - 353.
- Wood, D.H., 1993, "On wake modelling at high tip speed ratios", *Wind Engineering*, Vol. 16, pp. 291 - 303.

Wood, D.H., 1994, "Towards a theory for the runaway state of a horizontal-axis wind turbine", *Wind Engineering*, Vol. 18, pp. 93 - 103.

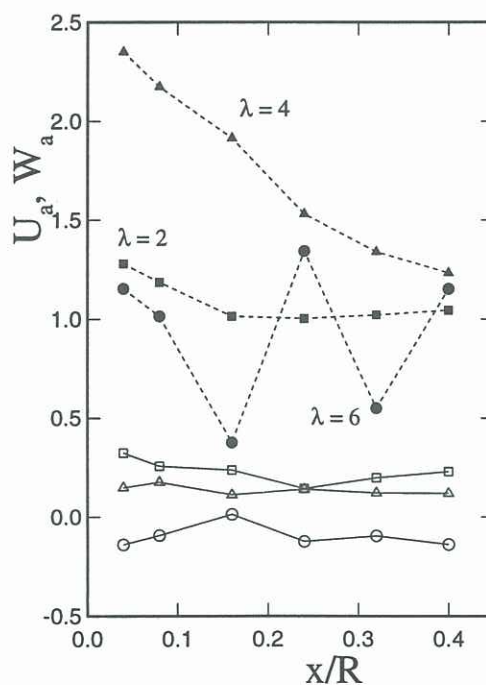


Figure 5. Downstream development of axial (U_a solid symbols) and binormal (W_a unfilled symbols) velocities of vortex cores. $\lambda = 2$, \square ; $\lambda = 4$, Δ ; $\lambda = 6$, \circ .